Experimental observation of surface acoustic wave Brillouin scattering in a small core photonic crystal fiber

Joël Cabrel Tchahame[a], Thibaut Sylvestre[a], Kien Phan Huy[a], Alexandre Kudlinski[b], Vincent Laude[a] and Jean-Charles Beugnot[a]

[a]Institut FEMTO-ST, Université de Bourgogne Franche-Comté, CNRS, Besanon, France
[b] PhLAM/IRCICA, CNRS-Université Lille 1, UMR 8523/USR 3380, F-59655 Villeneuve d'Ascq, France
Corresponding author: joelcabrel.tchahame@femto-st.fr

ABSTRACT

We report the experimental observation of surface acoustic wave Brillouin scattering (SAWBS) in a small-core photonic crystal fiber (PCF). These experimental results, supported by numerical simulations also show that the irregularities of the geometric structure could lead to the excitement of SAWBSs family around 5-6 GHz.

Keywords: Brillouin scattering, electrostriction force, photonic crytal fiber, surface acoustic wave, opto-acoustic

1. INTRODUCTION

Brillouin scattering is a nonlinear phenomenon due to interaction between light and acoustic waves.[1] Nowadays, the dynamic of Brillouin scattering in conventional fibers is well known, with many applications ranging from optical telecommunications, lasers to sensors.[2–4] However Brillouin scattering has recently been the subject of a renewed interest in thin optical fibers or micro/nano optical waveguides.[5–8] It has been shown that, a sub-wavelength scale PCF give rise to a 10 GHz-range multimode broadband Brillouin spectrum with a high onset threshold.[8] This mulimode ascpect to which is added the increase of the threshold, comes from the hybrid elastic waves generated in the PCF at this scale.[8] It has been also shown that light propagating in a subwavelength-diameter silica tapered fiber can generate surface acoustic waves (SAWs), because the strongly confined light senses the vibrations of the boundaries, leading to surface-localized light-sound interaction.[5] Such phenomenon is not observed in conventional telecom fibers because their core is much larger than the optical wavelength and the optical mode does not extend to the boundaries.

Even though SAWBSs can be generated with optical microfibers, they still limited by their short length (the length does not usually exceed a few tens of centimeters[9]) and a locked optical mode, important parameters to modulate the onset threshold of Brillouin scattering, and hence the SAWBSs. The PCFs offer both the ability to have long (>100 m) sub-wavelength waveguide and an adjustable geometric structure during manufacture to adapt the optical mode and shape the distribution of electrostrictive forces.

Here we report the observation of SAWBSs in a 99-m long single mode silica PCF. We also show that PCF's geometric structure greatly influences the shape of the spectrum.

2. EXPERIMENTAL MEASUREMENTS

The Figure 1 depicts the experimental setup used for SAWBSs measurements, based on heterodyne detection.[10] A continuous and narrow linewidth laser ($\sim$ 45 kHz) running at 1.55 μm was spitted in two beams by a 95/5 coupler. The first beam (5% of the pump) was amplified by an EDFA and launched in the PCF samples through a circulator. The backward Brillouin signal coming from the PCF was coupled to the second pump beam. The resulting beat signal was detected by a fast photodiode (12 GHz). The averaged Brillouin spectra were recorded with an electrical spectrum analyzer in the RF domain, around 6 GHz with a span of 2 GHz and 500 kHz of resolution. To achieve a better coupling ratio ($\sim$ 75 %) we have used a lensed fiber (FL) with a waist of 2.5

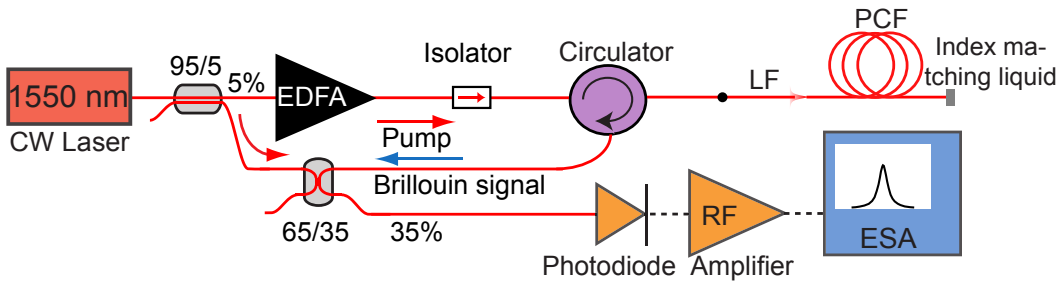

Figure 1. Experimental setup; CW: continuous wave, ESA: electrical spectrum analyzer, LF: lensed fiber, RF:radio-frequency.

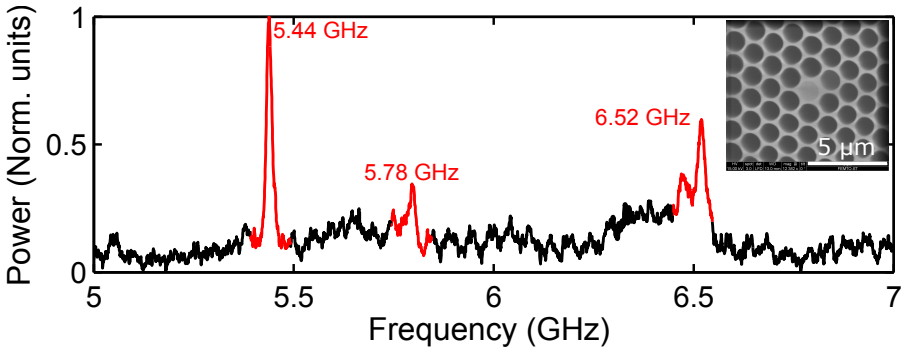

Figure 2. Experimental Brillouin spectrum, measured with a coupled power of 26.5 dBm. In inset we show the SEM image of the PCF cross scetion.

μm instead of a splicing coupling. A refractive index matching liquid were also added at the end of the PCF to minimize Fresnel reflections.

On the Figure 2 we show the experimental Brillouin scattering spectrum and the PCF's cross section SEM image, in insert. The core diameter is 1.57 μm, measured by considering the diameter of the inscribed circle in the center of the structure. The mean diameter of the holes closest to the core is 1.23 μm, and the picth is 1.3 μm. The PCF's linear losses, measured by cut-back technique are 0.062 dB.m^{-1}. We can clearly distinguish three main resonances peaks (located at 5.44 GHz, 5.78 GHz and 6.52 GHz). These peaks were identified as SAWBSs. To support this interpretation, we performed numerical simulations whose results are plotted on Figure 3. By using this relation: $V_{SAWBS} = \lambda\nu_B/2n_{eff}$ coming from the phase matching condition of Brillouin scattering, the SAW at 5.44 GHz is propagated with a velocity $\sim$ 3147 m.s^{-1}. Where $\lambda = 1.55$ μm is the optical wavelength; ν_B is the resonant Brillouin frequency; $n_{eff} = 1.3396$ is the effective refractive index, calculated by finite element method (FEM).

3. NUMERICAL CALCULATIONS

The theoretical Brillouin spectrum were obtained by computing (in FEM) the elastodynamic equation, driving by electrostrictive force. From that equation we have calculated the kinetic energy density due to the displacement inside the PCF. A perfect and a real geometric structure of the PCF have been considered for this calculations. The real geometry have the advantage to take into account the PCF's defects, which is not the case of a perfect geometry. This real geometric structure is directly extracted from the PCF's SEM image by a program of edge detection. However the perfect geometric structure remains necessary as it facilitated the interpretation of results from the modeling equations and shows the shape of the spectrum that we could get for a fiber fairly regular.

Further author information: (Send correspondence to joelcabrel.tchahame@femto-st.fr)

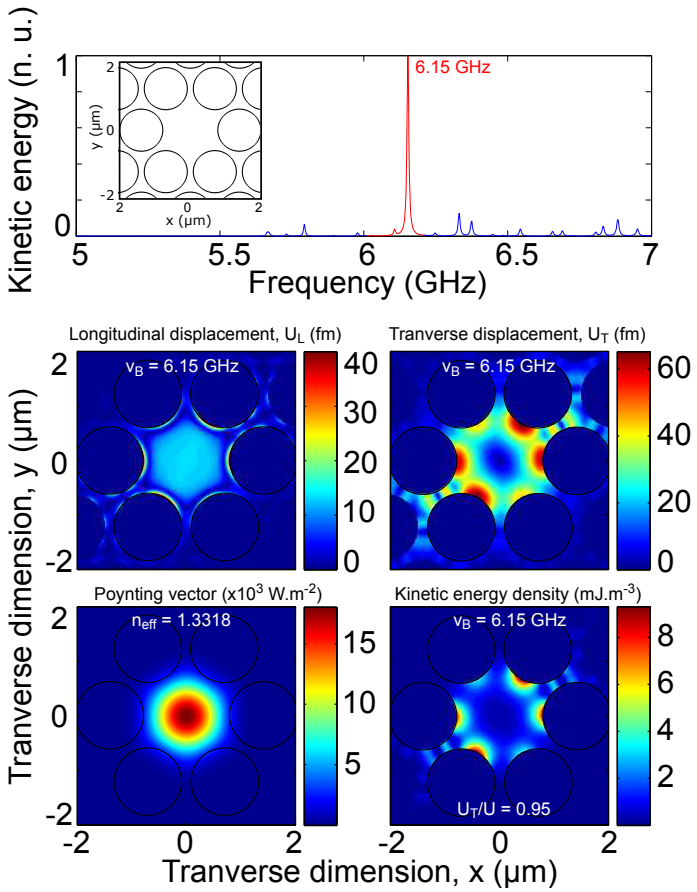

Figure 3. Numerical simulations of Brillouin scattering spectrum and the spatial distribution of displacements in the PCF by using a perfect geometry design.

The simulated elastodynamic equation is written as follows:

$$\rho \frac{\partial^2 u_i}{\partial t^2} - [C_{ijkl} u_{k,l}] = T^{es}_{ij,j}, \tag{1}$$

where ρ is the material density, u_i the displacement, C_{ijkl} the rank-4 elastic tensor of elastic contants. $T^{es}_{ij} = -\epsilon_0 \chi_{klij} E_k E^*_l$ is the electrostritive stress tensor, with rank-4 susceptibility tensor $\chi_{klij} = \epsilon_{km}\epsilon_{ln} p_{mnij}$ and p_{mnij} the elasto-optic tensor. ϵ_0 is the permitivity of vaccum. E_k and E_l are the pump and Brillouin Stokes fields with angular frequencies $\omega_{1,2}$ and axial wave vectors $k_{1,2}$. View the size of the PCF core (> 500 nm), the radiative pressure have been neglected.[5] We have also negleted the effect of optical birefringence $\sim 10^{-4}$. More details about this theoretical model used are given in.[11]

The resonances at 6 GHz-range are the ones of SAWBSs. We justify this by looking the spatial distribution of the diplacements and the kinetic energy density at a resonant frequency, as it is shown by simulations on the Figure 3. We clearly see a maximum concentration of kinetic energy density at the surface of the core, with a very shallow depth. Another important point is the ~ 0.95 ratio between the transverse displacement and the total displacement. Its reflects the fact that we excite hybrid acoustic waves, with predominantly transverse components. That is as well a key feature of the SAWs.

It is also important to point the diffence between the results in the case of perfect and real geometric structure. In the case of the perfect structure, we almost have a single SAWBS while the irregularities present in the real strcuture leads to the generation of a 6 GHz range SAWBSs family.

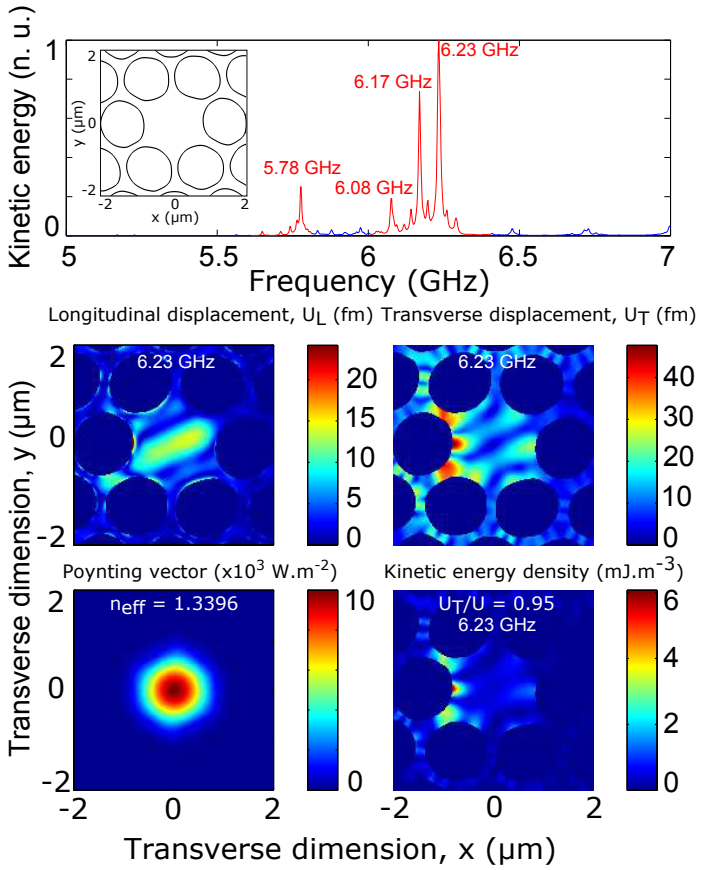

Figure 4. Numerical simulations of Brillouin scattering spectrum and the spatial distribution of displacements in the PCF by using a real geometry design.

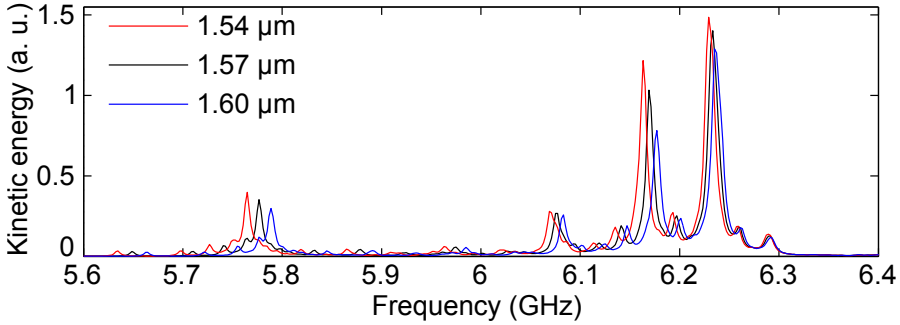

Figure 5. Numerical simulations of Brillouin scattering spectra for three differents core diameter.

We have also investigated by numerical simulations, the influence of core diameter on the SAWBSs. By variying the size (with a scale apply on the hole PCF's geometry structure) of the core diameter of about 30 nm, the SAWBSs frequency is shifted of 12 MHz. The results are plotted on Figure 5.

4. CONCLUSION

We have shown the generation of a new class of surface acoustic waves in a wavelength-scale silica PCF. Although there is a discrepancy of about 340 MHz between the theoretical (the one computed with the real geometric structure) and the experimental spectrum, we note a similarity. A very regular geometric structure appears to

be a very important factor for the generation of a SAWBS. Paradoxically, the irregularities of the geometry could also be useful for the generation of a SAWBSs family. This work may be a precursor in research dedicated to a simple and passive tuneability of SAWBSs components or multimodal SAWBSs.

ACKNOWLEDGMENTS

This work was supported by the University of Bourgogne Franche-Comté, the Labex Action program and the OASIS ANR (ANR-14-CE36-005-01).

REFERENCES

[1] Agrawal, G. P., [*Nonlinear fibers optics*], Academic press (2013).

[2] Kobyakov, A., Sauer, M., and Chowdhury, D., "Stimulated brillouin scattering in optical fibers," *Adv. Opt. Photon.* **2**, 1–59 (Mar 2010).

[3] Smith, S. P., Zarinetchi, F., and Ezekiel, S., "Narrow-linewidth stimulated brillouin fiber laser and applications," *Opt. Lett.* **16**, 393–395 (Mar 1991).

[4] Elooz, D., Antman, Y., Levanon, N., and Zadok, A., "High-resolution long-reach distributed brillouin sensing based on combined time-domain and correlation-domain analysis," *Opt. Express* **22**, 6453–6463 (Mar 2014).

[5] Beugnot, J.-C., Lebrun, S., Pauliat, G., Maillotte, H., Laude, V., and Sylvestre, T., "Brillouin light scattering from surface acoustic waves in a subwavelength-diameter optical fibre," *Nature communications* **5** (2014).

[6] Van Laer, R., Kuyken, B., Van Thourhout, D., and Baets, R., "Interaction between light and highly confined hypersound in a silicon photonic nanowire," *Nature Photonics* **9**(3), 199–203 (2015).

[7] Merklein, M., Kabakova, I. V., Büttner, T. F., Choi, D.-Y., Luther-Davies, B., Madden, S. J., and Eggleton, B. J., "Enhancing and inhibiting stimulated brillouin scattering in photonic integrated circuits," *Nature communications* **6** (2015).

[8] Dainese, P., Russell, P. S. J., Joly, N., Knight, J., Wiederhecker, G., Fragnito, H. L., Laude, V., and Khelif, A., "Stimulated brillouin scattering from multi-ghz-guided acoustic phonons in nanostructured photonic crystal fibres," *Nature Physics* **2**(6), 388–392 (2006).

[9] Kang, M. S., Brenn, A., Wiederhecker, G. S., and Russell, P. S., "Optical excitation and characterization of gigahertz acoustic resonances in optical fiber tapers," *Applied Physics Letters* **93**(13) (2008).

[10] Beugnot, J. C., Sylvestre, T., Alasia, D., Maillotte, H., Laude, V., Monteville, A., Provino, L., Traynor, N., Mafang, S. F., and Thévenaz, L., "Complete experimental characterization of stimulated brillouin scattering in photonic crystal fiber," *Opt. Express* **15**, 15517–15522 (Nov 2007).

[11] Beugnot, J.-C. and Laude, V., "Electrostriction and guidance of acoustic phonons in optical fibers," *Phys. Rev. B* **86**, 224304 (Dec 2012).